J. Fluid Mech. (1972), *vol.* 54, *part* 4, *pp.* 665–678
Printed in Great Britain

The solution of sharp-cone boundary-layer equations in the plane of symmetry

By JOHN W. MURDOCK
The Aerospace Corporation, San Bernardino, California

(Received 16 June 1971 and in revised form 13 April 1972)

A detailed study has been made of the solutions to cone boundary-layer equations in the symmetry plane in order to increase understanding of the mathematical nature and physical meaning of these solutions. A typical set of symmetry-plane solutions is presented. Included in this set are various solution branches not previously published. A double-valued solution curve is found which has not been studied prior to this time except at one trivial point. The extension of an existing solution branch through a removable singular point has also been accomplished. The solutions presented are categorized according to whether they are dependent on or independent of the boundary layer outside the symmetry plane. The region in which no solutions to the usual symmetry-plane equations exist is examined. Solutions in which the usual boundary-layer model predicts that conservation of mass is not satisfied at the symmetry plane are discussed. Non-analytical behaviour at the symmetry plane is also investigated. In both of these cases a boundary region exists at the symmetry plane.

1. Introduction

The purpose of this paper is to investigate, very generally, the behaviour of the solutions to the cone boundary-layer equations in the vicinity of the plane of symmetry. The boundary-layer equations for a sharp cone at an angle of attack were first derived by Moore (1951). The solutions considered herein are the first-order inner expansions of the Navier–Stokes equations as discussed, for example, by Van Dyke (1964, p. 126). Higher-order terms in the expansion are not considered. Consistent with this is the neglect of the vortical sublayer on the body and the vortical singularity shown by Ferri (1950) to occur in the leeward symmetry plane. When the boundary and vortical layers are of comparable thickness there is, of course, an interaction, but this interaction belongs to higher order boundary-layer theory (Van Dyke 1969) and, therefore, neglecting it is consistent with the restriction to the first-order expansion of the Navier–Stokes equations.

The solutions to the cone boundary-layer equations in the symmetry plane have been discussed by Moore (1953, 1956), by Reshotko (1957) and by Cheng (1961). Trella & Libby (1965) and Libby & Liu (1968) considered a more general plane-of-symmetry problem in which there is a pressure gradient along the plane. The complete boundary-layer equations have been integrated numerically by Vvedenskaya (1966), Boericke (1969) and Dwyer (1971).

In § 2, the complete cone boundary-layer equations (Moore 1951), as well as the usual symmetry-plane equations (Moore 1953), are given. Section 3 summarizes the results of a numerical study, the intent of which was to obtain as many solutions to the symmetry-plane equations as possible. Solutions in agreement with published solutions are found. A new solution branch for k positive is presented, as well as a new double-valued branch for negative k. At all points in k space at which solutions are found the solution curves are double-valued. In certain regions of k space, no solutions were found, however. The domain of dependence of the symmetry-plane solutions presented is discussed. Section 4 discusses the behaviour of published solutions to the complete boundary-layer equations in the vicinity of the symmetry plane when the behaviour is non-analytic at this point. Two types of non-analytic behaviour are discussed.

2. Derivation of equations

The three-dimensional boundary-layer equations for a sharp cone, written in terms of x, the co-ordinate along a cone generator, ϕ, the cone azimuthal angle, and y, the co-ordinate normal to the cone surface, are the continuity equation

$$(\rho u r)_x + (\rho v r)_y + (\rho w)_\phi = 0, \tag{1}$$

the x-momentum equation

$$u u_x + v u_y + \frac{w}{r} u_\phi - \frac{w^2}{r}\frac{dr}{dx} = \frac{1}{\rho}(\mu u_y)_y, \tag{2}$$

the ϕ-momentum equation

$$u w_x + v w_y + \frac{w}{r} w_\phi + \frac{uw}{r}\frac{dr}{dx} = -\frac{1}{\rho r}\frac{dp}{d\phi} + \frac{1}{\rho}(\mu w_y)_y \tag{3}$$

and the energy equation, in terms of the total enthalpy H,

$$u H_x + v H_y + \frac{w}{r} H_\phi = \frac{1}{\rho}(\mu H_y)_y. \tag{4}$$

It has been assumed that the Prandtl number is unity. If it is further assumed that the fluid is a perfect gas and that the viscosity varies as the absolute temperature, then the preceding equations may be simplified by introducing the following quantities. A new independent variable η is defined as

$$\eta = \left[\frac{3u_e}{2\rho_e \mu_e x}\right]^{\frac{1}{2}} \int_0^y \rho \, dy. \tag{5}$$

The definitions of the new dependent variables are

$$f_\eta = u/u_e, \quad g_\eta = w/w_e, \tag{6), (7}$$

$$\Theta = (H - H_w)/(H_e - H_w). \tag{8}$$

Substitution of (5)–(8) into (1)–(4) yields

$$f_{\eta\eta\eta} + f f_{\eta\eta} + \frac{1}{3\sin\theta}\frac{w_e}{u_e}\left[\frac{2}{w_e}\frac{dw_e}{d\phi} + \frac{1}{p}\frac{dp}{d\phi} - \frac{w_e}{u_e}\sin\theta\right] g f_{\eta\eta} - \frac{2}{3}\left(\frac{w_e}{u_e}\right)^2 [g_\eta f_\eta - g_\eta^2] = \frac{2}{3\sin\theta}\frac{w_e}{u_e}[g_\eta f_{\eta\phi} - g_\phi f_{\eta\eta}], \tag{9}$$

$$g_{\eta\eta\eta}+fg_{\eta\eta}+\frac{1}{3\sin\theta}\frac{w_e}{u_e}\left[\frac{2}{w_e}\frac{dw_e}{d\phi}+\frac{1}{p}\frac{dp}{d\phi}-\frac{w_e}{u_e}\sin\theta\right]gg_{\eta\eta}+\frac{2}{3}\left(\frac{\rho_e}{\rho}-f_\eta g_\eta\right)$$
$$+\frac{2}{3\sin\theta}\frac{1}{u_e}\frac{dw_e}{d\phi}\left[\frac{\rho_e}{\rho}-g_\eta^2\right]=\frac{2}{3\sin\theta}\frac{w_e}{u_e}[g_\eta g_{\eta\phi}-g_\phi g_{\eta\eta}], \tag{10}$$

$$\Theta_{\eta\eta}+f\Theta_\eta+\frac{1}{3\sin\theta}\frac{w_e}{u_e}\left[\frac{2}{w_e}\frac{dw_e}{d\phi}+\frac{1}{p}\frac{dp}{d\phi}-\frac{w_e}{u_e}\sin\theta\right]g\Theta_\eta$$
$$=\frac{2}{3\sin\theta}\frac{w_e}{u_e}[g_\eta\Theta_\phi-g_\phi\Theta_\eta]. \tag{11}$$

The density ratio ρ_e/ρ appearing in (10) is given by

$$\frac{\rho_e}{\rho}=\left[1+\frac{u_e^2+w_e^2}{2h_e}\right]\left[\Theta+\frac{H_w}{H_e}(1-\Theta)\right]-\frac{u_e^2}{2h_e}f_\eta^2-\frac{w_e^2}{2h_e}g_\eta^2. \tag{12}$$

The boundary conditions are

$$\left.\begin{aligned} f=f_\eta=g=g_\eta=\Theta=0 \quad &\text{for} \quad \eta=0,\\ f_\eta=g_\eta=\Theta=1 \quad &\text{as} \quad \eta\to\infty. \end{aligned}\right\} \tag{13}$$

In the plane of symmetry the preceding equations simplify considerably. In this plane, w_e is zero and, thus, if the dependent variables and their derivatives remain finite (9), (10), and (11) reduce to

$$f_{\eta\eta\eta}+(f+kg)f_{\eta\eta}=0, \tag{14}$$

$$g_{\eta\eta\eta}+(f+kg)g_{\eta\eta}+\frac{2}{3}\left(\frac{\rho_e}{\rho}-f_\eta g_\eta\right)+k\left(\frac{\rho_e}{\rho}-g_\eta^2\right)=0, \tag{15}$$

$$\Theta=f_\eta, \tag{16}$$

where the parameter k defined by Moore (1953) has been introduced:

$$k=\frac{2}{3u_e\sin\theta}\frac{dw_e}{d\phi}. \tag{17}$$

3. Solutions to the plane-of-symmetry equations

The solutions presented herein were generated using a Runge–Kutta numerical-integration technique, with the symmetry-plane equations treated as an initial-value problem. It was thus necessary to iterate on $f_{\eta\eta}$ and $g_{\eta\eta}$ at the wall in order to satisfy the edge boundary conditions. The iteration converged very nicely except for the new solution branch found for positive k. (The solutions are discussed in detail in the succeeding paragraphs.) On the branch where difficulties were encountered, it was possible to obtain convergence if small enough steps in k were taken from one solution to the next. Consequently, all the solutions to be discussed were generated in the same manner, although it is clear in retrospect that a more sophisticated numerical technique is desirable for this problem. A conservative estimate of the accuracy of the solutions generated is five significant figures.

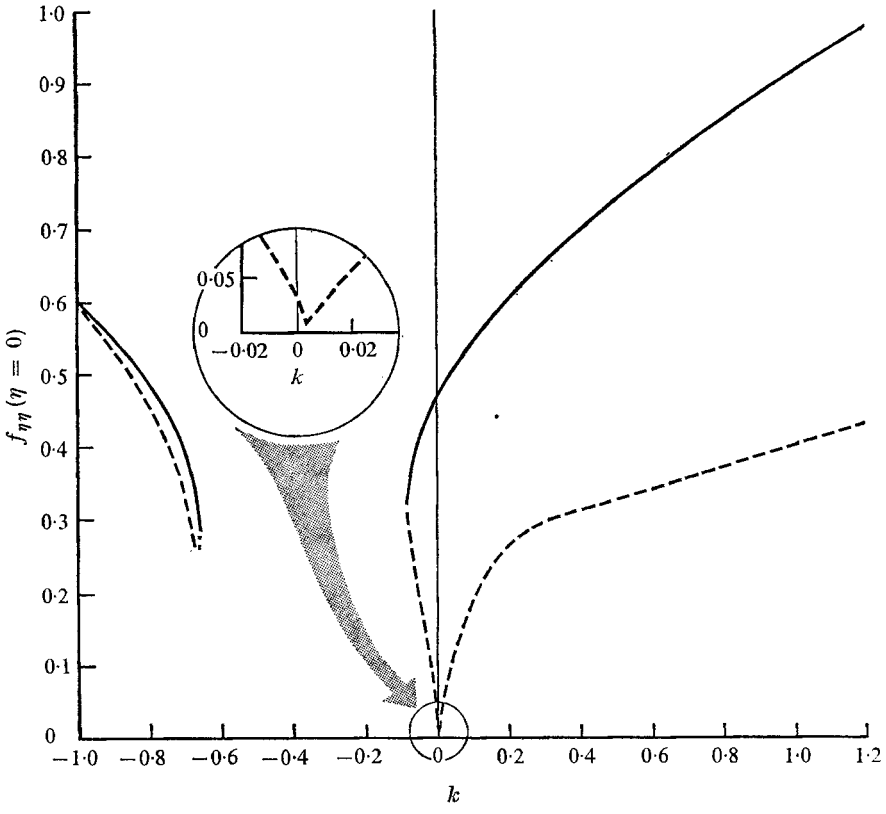

FIGURE 1. Values of $f_{\eta\eta}(\eta = 0)$ in plane of symmetry. $H_w/H_e = 0{\cdot}4$ and $u_e^2/2h_e = 8{\cdot}0$ for this and figures 2–6.

Moore (1953) investigated the asymptotic behaviour of solutions to the symmetry-plane equations and found two asymptotic solutions, one with algebraic behaviour and one with exponential behaviour. The solution with algebraic behaviour only decays if $k < -\frac{1}{3}$. For $k < -1$ neither solution decays and, therefore, no solutions exist in this region. In a later paper, Moore (1956) states that the solutions which decay algebraically must be rejected on physical grounds because they do not have a finite displacement thickness. The solutions presented in this section all exhibit exponential decay at infinity and, therefore, have finite integral thicknesses. A generalization of the method used by Libby (1967) was used to check the numerical solutions for the desired asymptotic behaviour.

To obtain solutions to the cone boundary-layer equations in the plane of symmetry, (14)–(16), three parameters must be specified. The first of these, k, appears explicitly and is defined by (17). It is this parameter which is of primary interest here. The remaining two parameters appear in expression (12) for ρ_e/ρ and are the ratio H_w/H_e of the wall to free-stream total enthalpy and a parameter related to the square of the edge Mach number, $u_e^2/2h_e$. It is not the intent of this paper to provide an extensive catalogue of solutions to the plane-of-

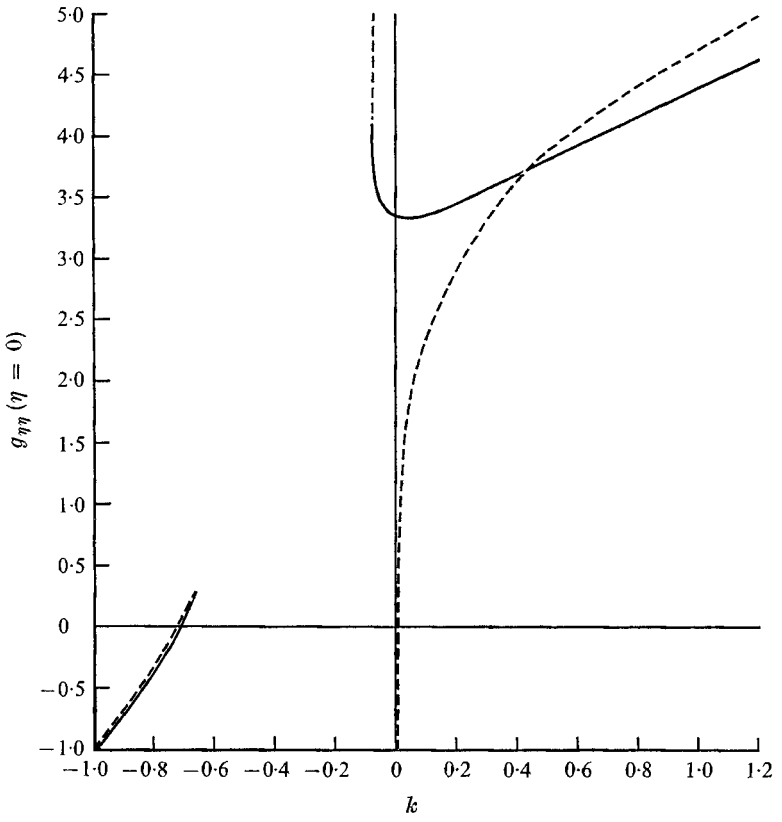

FIGURE 2. Values of $g_{\eta\eta}(\eta = 0)$ in plane of symmetry.

symmetry equations.† Instead, a typical set of solutions with the parameter k variable and the other two parameters held constant will be presented to illustrate the behaviour of the velocity profiles as a function of k. A value of $H_w/H_e = 0{\cdot}4$ and a value of $u_e^2/2h_e = 8{\cdot}0$ have been used in the results reported in the succeeding paragraphs.

Figure 1 shows the wall values of $f_{\eta\eta}$ (and $\Theta_\eta = f_{\eta\eta}$) plotted versus the parameter k for the plane-of-symmetry solutions. In figure 1, one branch of the curve is solid and the other dashed; in succeeding figures this coding is retained so that corresponding curves may be easily identified. The behaviour of the wall values of $g_{\eta\eta}$ is shown in figure 2. Most of the published solutions to (14) and (15) are for k positive and correspond to the solid curve in figures 1 and 2. As this curve is followed into negative k space the branch point found by Cheng (1961) is approached. The behaviour of the solution as $k = 0$ is approached on the dashed branch has apparently not been characterized previously. The boundary layer thickens, $f_{\eta\eta}$ decreases and g approaches infinity like k^{-1}. This singular behaviour may be removed by defining a new variable

$$h = kg. \tag{18}$$

† A paper by Roux (1972), published while this paper was being refereed, presents additional solutions and interpretation of the solutions considered herein.

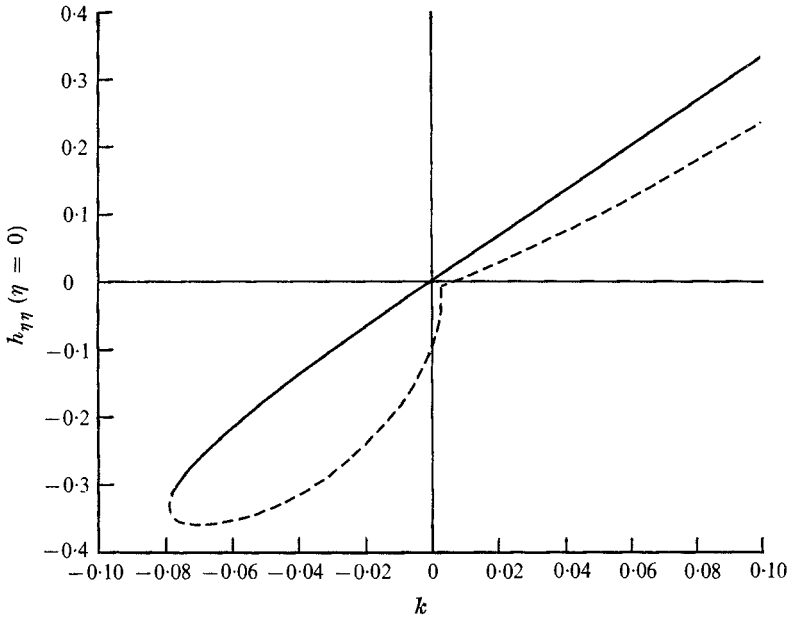

FIGURE 3. Values of $h_{\eta\eta}$ ($\eta = 0$) in plane of symmetry.

Thus, (14) and (15) become

$$f_{\eta\eta\eta} + (f+h) f_{\eta\eta} = 0, \tag{19}$$

$$h_{\eta\eta\eta} + (f+h) h_{\eta\eta} + (k+\tfrac{2}{3}) k(\rho_e/\rho) - \tfrac{2}{3} f_\eta h_\eta - h_\eta^2 = 0, \tag{20}$$

with boundary conditions

$$\left.\begin{aligned} f = f_\eta = h = h_\eta = 0 \quad &\text{for} \quad \eta = 0, \\ f_\eta = 1, \quad h_\eta = k \quad &\text{as} \quad \eta \to \infty. \end{aligned}\right\} \tag{21}$$

Using this formulation, a second and new solution at $k = 0$ may be obtained. This solution is an 'incompressible' solution, and the values of $f_{\eta\eta}$ and $h_{\eta\eta}$ (0·0335 and −0·0931, respectively) are common to all curves, regardless of the values of the wall temperature and edge Mach number. Figure 3 shows the variation of $h_{\eta\eta}$ at the wall with k in the region of k space in which use of h rather than g is convenient. Note that the velocity w is well behaved as $k \to 0$ on this (the dashed) branch, even though g_η is singular. Combination of (7), (17) and (21) with the following expression valid for small ϕ,

$$w_e = (dw_e/d\phi)\,\phi, \tag{22}$$

gives

$$w = \tfrac{3}{2} \sin\theta\, u_e \phi h_\eta + \text{terms of higher order in } \phi. \tag{23}$$

Thus w is finite (going to zero with ϕ) for finite h_η. For $k = 0$, w_e goes to zero like ϕ^3 and thus the w-velocity profile becomes one of pure overshoot.

This new (dashed) solution branch returns to positive k space, undergoing a rather abrupt change in direction at a value of k of about 0·0028. (See figures 1 and 3.) A careful study of the solutions in this region has shown that the slope of the curves is continuous. That is to say, there is neither a cusp nor an intersection

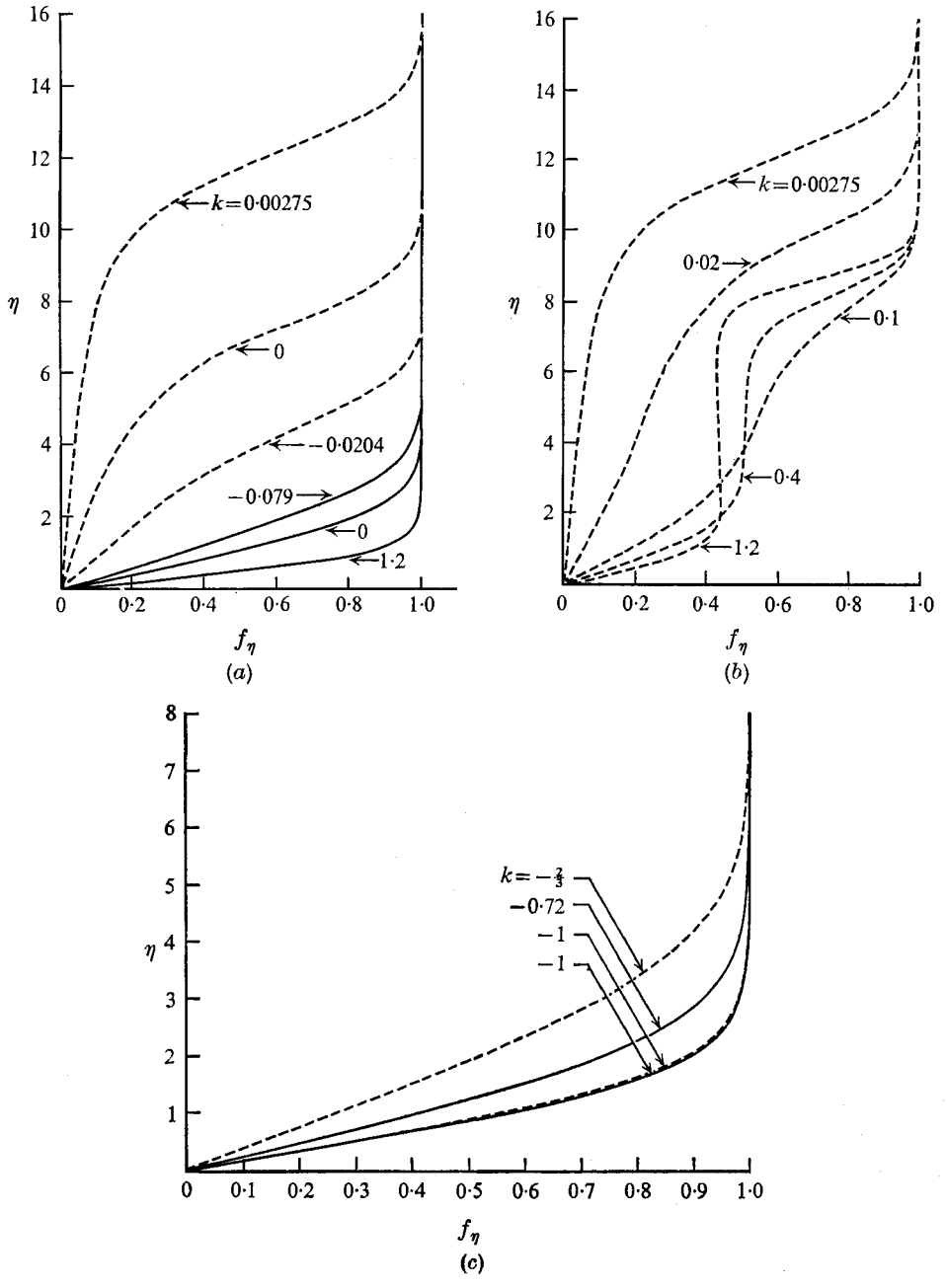

FIGURE 4. Typical u-velocity (f_η) profiles.

of two separate curves at this point. Following the curves out in positive k space reveals no further drastic changes.

A second double-valued solution curve (figures 1 and 2), which, except at one point, has apparently never been discussed, has been found for values of k between $-0{\cdot}6656$ and -1. The exceptional point is $k = -\frac{2}{3}$ and the solution there may be

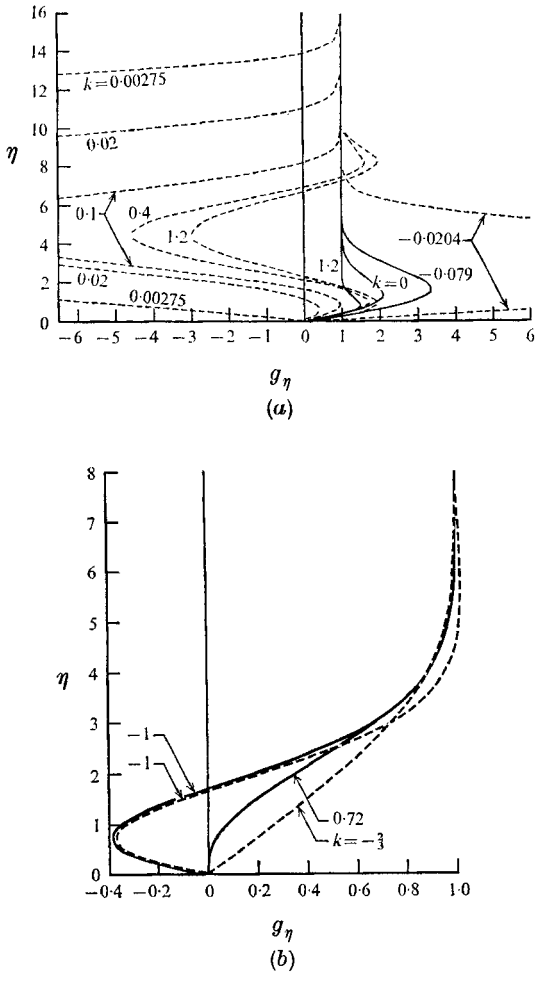

FIGURE 5. Typical w-velocity (g_η) profiles.

obtained from the flat-plate solution of Moore (1951). At this point f and g are equal and the solution is Blasius-like. There is also a second solution at $k = -\frac{2}{3}$ with $f \neq g$. Note that for both the $k = -\frac{2}{3}$ solutions the density terms drop out of (14) and (15), and these two 'incompressible' points are common to any curve (figures 1 and 2). (P. A. Libby, in a private communication, has indicated that at least two more solutions exist in this region of k space.)

Typical velocity profiles associated with the solutions discussed above are given in figures 4, 5, and 6. The evolution of the velocity profiles as k varies from positive to negative, along the solid curve in figures 1 and 2, and back to positive, along the dashed curve, will be discussed. The behaviour of the u-velocity profiles shown in figure 4 (a) changes little with k as k decreases from 1·2 to −0·079, and is always very much like that of a Blasius profile. When the branch point has been passed changes begin to occur much more rapidly. In figure 4 (a) the u-velocity profile becomes more and more inflected until it looks very much like a shear

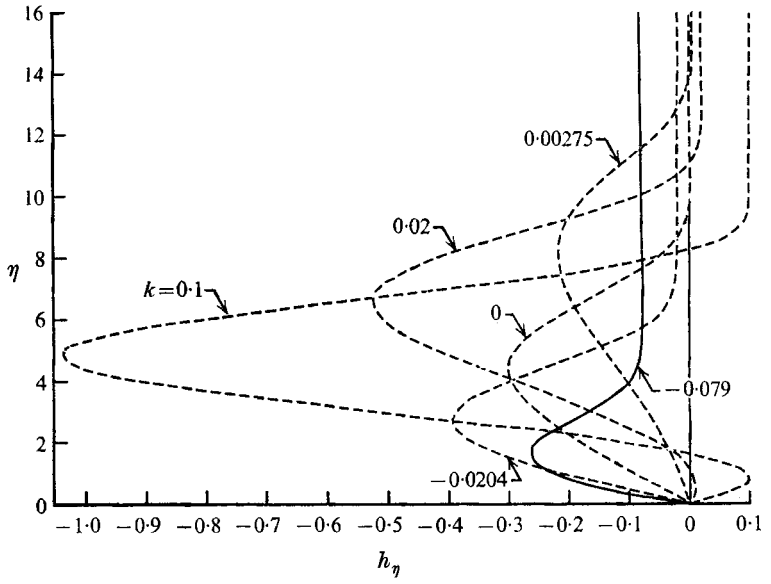

FIGURE 6. Typical w-velocity (h_η) profiles.

layer profile, at $k = 0{\cdot}00275$. As k approaches zero, g_η (figure 5(a)) goes to infinity and, therefore, the w-profiles for small k are best shown in terms of h_η as in figure 6. As k is increased beyond 0·00275, the tendency for the boundary layer to thicken is reversed. In figure 4(b) the u-velocity is seen to evolve into a profile with a rather extensive constant-velocity region. All the positive-k solutions on the dotted branch have reverse flow in the ϕ direction. The evolution of g_η from a profile which is predominately a reverse flow to a forward–reverse–forward profile is shown in figure 5(a).

The velocity profiles associated with the left-hand solution branch do not change nearly so much as those discussed above. It is obvious from inspection of (14) and (15) that, for $k = -\frac{2}{3}$, one solution for both f_η and g_η is Blasius-like. This solution is shown in figures 4(c) and 5(b) along with solutions for other typical values of k. All the u-velocity profiles shown in figure 4(c) are very similar, and there is a very small difference between any two solutions at the same value of k. The w-velocity solutions evolve from the Blasius-like solution to a solution with a substantial reverse flow near the wall. As k approaches minus one, the dashed velocity profiles overshoot and approach unity from above while the solid ones asymptote from below. This appears to be the only significant difference between the two branches of this solution curve.

Because of the non-uniqueness of the solutions in k space, it is useful to look for physical or mathematical differences between the solution branches. It has been found that on the solid branch of the right-hand solution curve the inequality

$$f + kg > 0 \tag{24}$$

is satisfied for any value of η. On the dotted right-hand solution branch, the inequality (24) is satisfied in part of the boundary layer and violated in the rest

of the layer. At the branch point the inequality becomes an equality on the body. Although (24) characterizes the difference between the two branches of the right-hand curve, it does not do so for the left-hand one. Except at $k = -1$, $\eta \to \infty$, all the solutions on the left-hand curve satisfy (24) everywhere.

The physical significance of (24) is as follows. For those symmetry-plane solutions which satisfy (24), the streamlines which enter the edge of the boundary-layer asymptote onto the body in the sense that the streamlines cross lines of constant η. For those solutions which do not satisfy (24) everywhere, the streamlines in the symmetry plane enter the boundary layer and asymptote onto some line of constant η. The portion of the boundary layer below the asymptote is, therefore, occupied by fluid which has entered the symmetry plane from the side.

The domain of dependence of three-dimensional boundary layers has been investigated by Wang (1971). He concluded that the origin of the streamlines determines the domain of dependence of the boundary layer at a given body location. In the present case, therefore, it is clear that the solid branch of the right-hand solution and all the left-hand solutions have only the symmetry plane as the domain of dependence, since all of the boundary-layer streamlines originate in this plane. The right-hand dashed solutions are such that a finite region in the boundary layer is occupied by fluid which entered the symmetry plane from the side, and therefore solutions on this branch are in the domain of dependence of some region adjacent to the symmetry plane as well as the symmetry plane.

Wang (1971) argues that the domain of dependence of the three-dimensional boundary-layer equations is determined by the sub-characteristics of the equations and he shows that the sub-characteristics are streamlines. The sub-characteristics of the system of equations (9)–(11) are the streamlines in ϕ, η space and are given by

$$\frac{d\phi}{\phi} = \frac{-kg_\eta d\eta}{[f+kg+O(\phi^2)]}. \tag{25}$$

It is obvious from inspection of (25) that there is a node-type singularity at $\phi = 0$, where $f+kg = 0$. Thus, when inequality (24) is not satisfied everywhere, the streamlines or sub-characteristics actually enter the symmetry plane at the singular points of (25). Dashed-branch solutions on the right-hand curve have one singular point for values of $k < 0{\cdot}0030$ (approximately the turning point in figure 1). At larger values of k, there are two singular points of (25) in the dashed-branch boundary layer.

4. Non-analytic behaviour at the symmetry plane

It is of interest to investigate the behaviour of the boundary-layer solutions at the symmetry plane in the region $-0{\cdot}665 < k < -0{\cdot}079$, in which no solutions to the usual equations were found. The mathematical reason for the non-existence of solutions to the symmetry-plane equations will not be investigated; rather, it is assumed that integrating the complete boundary-layer equations from a windward to a leeward plane gives a unique result at the leeward plane, whether solutions to the usual symmetry-plane equations exist or not.

Boericke (1969) and Dwyer (1971) have integrated the complete equations around the cone in regions where symmetry-plane solutions are non-existent and have reported very large values of g_η as the leeward symmetry plane is approached. Boericke (1969) published a family of g_η profiles very near the leeward symmetry plane. A careful study of these results indicates that g_η is singular like ϕ^{-1} (where $\phi = 0$ is the leeward symmetry plane). The usual symmetry-plane equations are obtained from the complete equations by assuming that g is finite; thus the singular solutions do not satisfy (14), (15) and (16).

Since w_e ordinarily goes to zero like ϕ at the symmetry plane and if g is $O(\phi^{-1})$, then, from the definition (7), w is non-zero at the symmetry plane. Thus, the result is obtained that an integration of the usual boundary-layer equations around the cone may predict a finite ϕ velocity into the symmetry plane from both sides. This predicted behaviour cannot exist in reality. Because the complete equations are parabolic with ϕ, the time-like direction, no boundary condition may be imposed at the leeward symmetry plane to correct this behaviour (if w is from windward to leeward). The physically relevant solution at the symmetry plane, in this case, must be obtained by inserting a boundary region at the symmetry plane. The derivation of the governing equations in this boundary region is beyond the scope of the present paper. However, it is expected that the derivation would follow lines similar to those taken by Rubin (1966) for corner flow and Stewartson (1961) for flow past a quarter-infinite plate.

If the usual boundary-layer equations predict a finite w-velocity at the leeward symmetry plane, then the maximum velocity $w_{\max}$ should have a series expansion

$$w_{\max}/u_e(\phi = 0) = c_0 + c_1\phi + c_2\phi^2 + \dots \quad . \tag{26}$$

Using the solutions plotted in figure 5.7 of Boericke's (1969) thesis, figure 7 has been constructed. The maximum velocity into the leeward symmetry plane for this case is less than 0·1 per cent of the edge velocity.

To summarize, the numerical solutions of Boericke (1969) and Dwyer (1971) indicate that when solutions to the usual symmetry plane equations do not exist, the complete boundary-layer equations predict finite w-velocities at the leeward symmetry plane. The evidence is not sufficient to determine whether or not other types of behaviour are also possible.

The solutions discussed in the preceeding paragraphs are characterized by finite and discontinuous w-velocities at the symmetry plane. Moore (1951) has solved the usual boundary-layer equations on a flat plate with two intersecting straight lines as a leading edge. This solution is an exact solution of (9)–(12) and is sufficiently well behaved to satisfy (14)–(16) at the symmetry plane. Moore's (1951) solution does, however, have discontinuities in the velocity derivatives with respect to ϕ at the symmetry plane and, therefore, a boundary region must be inserted to model the flow correctly. Moore's solution is for $k = -\frac{2}{3}$; it is of interest to determine where else in k space this type of discontinuity may exist. To do this, we expand the dependent variables in series about $\phi = 0$ and substitute these into (9)–(12). Equations (14)–(16) are obtained by collecting terms of zero order in ϕ; collecting terms of order ϕ defines an eigenvalue problem. The eigenvalues are the points in k space where the Moore-type non-analytic behaviour

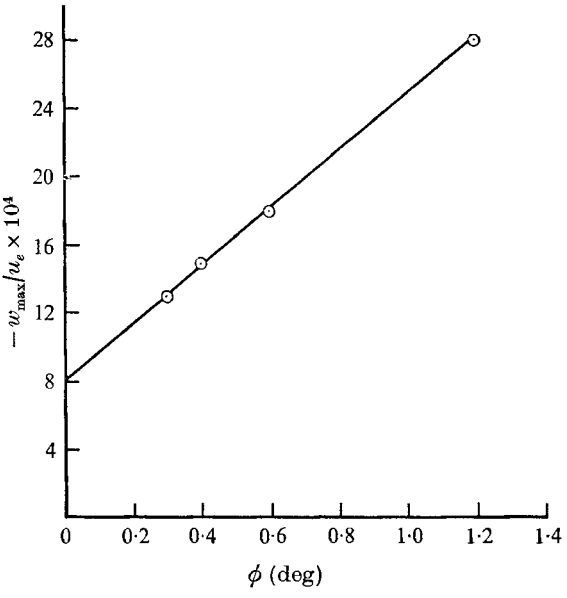

FIGURE 7. Maximum ϕ-velocity near the leeward plane of symmetry for 7·5° cone at Mach 3·1; $\alpha = 1{\cdot}5°$. ⊙, Boericke (1969); ——, straight line drawn through the points.

Eigenvalue	Solution branch	Eigenvalue	Solution branch
−0·0666	Solid	−0·671	Solid
−0·0228	Dashed	−0·667	Solid
0·00204	Dashed	$-\frac{2}{3}$	Dashed
0·00409	Dashed	−0·679	Dashed
0·302	Dashed	−0·725	Dashed
−0·860	Solid		

TABLE 1. Eigenvalues in k space for $H_w/H_e = 0{\cdot}4$ and $u_e^2/2h_e = 8{\cdot}0$

may occur. The actual eigenvalues, corresponding to the family of symmetry-plane solutions given in § 3, are presented in table 1.

The two situations in which a boundary region is required at the symmetry plane differ as follows. In the first case, the boundary region smoothes out discontinuities in w, g_η is infinite and the solutions do not satisfy (14)–(16) as $\phi \to 0$ outside the boundary region. In the second case, the boundary region smoothes out discontinuities in certain shear stress components, g_η is finite and the solutions for $\phi \to 0$ outside the boundary region satisfy (14)–(16). Thus, in those regions of k space where no solution to (14)–(16) exists, a boundary region is apparently required to model the flow at the symmetry plane correctly. In those regions of k space where solutions to (14)–(16) do exist these solutions correctly model the flow at the symmetry plane, except at certain discrete points, such as those given in table 1. At these points in k space, a boundary region is required to model the flow at the symmetry plane adequately, if the magnitude of the corresponding eigenfunction is non-zero. If the magnitude of the eigenfunction is zero then no boundary region is required.

5. Discussion and conclusions

A detailed study of the plane-of-symmetry equations has produced solution branches not previously published. The double-valued solution curve for $-1 < k < -0{\cdot}6656$ has not been studied prior to this time, although one solution on this curve at $k = -\frac{2}{3}$ was first given by Moore (1951). In addition, a completely new solution curve has been found for k positive. These solutions are interesting because they are not only exact solutions in the symmetry plane, but they are also expected to indicate, in a qualitative sense, the kinds of velocity profiles to be found outside the symmetry plane.

The conditions for the plane-of-symmetry boundary layer to be independent of or dependent upon the out-of-plane flow have been given. The branch point on the right-hand curve divides the solutions which are in the domain of dependence of only the symmetry plane from those in the domain of dependence of the out-of-plane flow. The existence of discontinuous velocity derivatives at the plane of symmetry is shown to be a defect in the usual boundary-layer model. The behaviour of published complete boundary-layer solutions in the region where the symmetry-plane solutions do not exist has been examined. It is concluded that the boundary-layer model has a lower order defect in this case and that the w velocity is discontinuous.

The boundary-layer equations have been found to give physically unsatisfactory solutions in the leeward symmetry plane when the velocity or the derivatives of the velocity are discontinuous. Very similar situations may be found in the literature. Viscous flow past a quarter-infinite plate has been considered by Stewartson (1961) and corner flow by Rubin (1966); in each case a system of equations, valid in the corresponding boundary region, was derived. It is presumed that the method of matched asymptotic expansions (see, for example, Van Dyke 1964, p. 121) could also be applied to the present problem and a boundary region formulation valid near the symmetry plane produced. This technique would resolve the problem associated both with discontinuous velocities and discontinuous derivatives which have been found to occur at the leeward symmetry plane.

Although all the results presented herein are specifically for a sharp cone, similar behaviour and problems with the boundary-layer model should be expected along the symmetry planes of more general three-dimensional bodies.

REFERENCES

BOERICKE, R. R. 1969 The laminar boundary layer on a cone at incidence in supersonic flow. Ph.D. thesis, Polytechnic Institute of Brooklyn. (See also 1970 *A.I.A.A.* 8th *Aerospace Sciences Meeting Paper*, 70–48.)

CHENG, H. K. 1961 The shock layer concept and three-dimensional hypersonic boundary layers. *Cornell Aero. Lab. Rep.* AF-1285-A-3.

DWYER, H. A. 1971 Boundary layer on a hypersonic sharp cone at small angle of attack. *A.I.A.A. J.* **9**, 277–284.

FERRI, A. 1950 Supersonic flow around circular cones at angles of attack. *N.A.C.A. Tech. Note.* no. 2236.

LIBBY, P. A. 1967 Heat and mass transfer at a general three-dimensional stagnation point. *A.I.A.A. J.* **5**, 507–517.

LIBBY, P. A. & LIU, T. M. 1968 Some similar laminar flows obtained by quasi-linearization. *A.I.A.A. J.* **6**, 1541–1548.

MOORE, F. K. 1951 Three-dimensional compressible laminar boundary-layer flow. *N.A.C.A. Tech. Note*, no. 2279.

MOORE, F. K. 1953 Laminar boundary layer on cone in supersonic flow at large angle of attack. *N.A.C.A. Rep.* no. 1132. (See also 1952 *N.A.C.A. Tech. Note*, no. 2844.)

MOORE, F. K. 1956 Three-dimensional boundary layer theory. *Advances In Applied Mechancis*, **4**, 159–228.

RESHOTKO, E. 1957 Laminar boundary layer with heat transfer on a cone at angle of attack in a supersonic stream. *N.A.C.A. Tech. Note*, no. 4152.

ROUX, B. 1972 Supersonic laminar boundary layer near the plane of symmetry of a cone at incidence. *J. Fluid Mech.* **51**, 1–14.

RUBIN, S. G. 1966 Incompressible flow along a corner. *J. Fluid Mech.* **26**, 97–110.

STEWARTSON, K. 1961 Viscous flow past a quarter-infinite plate. *J. Aerospace Sci.* **28**, 1–10.

TRELLA, M. & LIBBY, P. A. 1965 Similar solutions for the hypersonic boundary layer near a plane of symmetry. *A.I.A.A. J.* **3**, 75–83.

VAN DYKE, M. 1964 *Perturbation Methods in Fluid Mechanics*. Academic.

VAN DYKE, M. 1969 Higher-order boundary layer theory. *Ann. Rev. Fluid Mech.* **1**, 265–292.

VVEDENSKAYA, N. D. 1966 Calculation of the boundary layer arising in a flow about a cone under an angle of attack. *Zh. vychisl. Mat. mat. Fizl.* **6**, 304–312.

WANG, K. C. 1971 On the determination of the zones of influence and dependence for three-dimensional boundary-layer equations. *J. Fluid Mech.* **48**, 397–404.